doi:10.1093/brain/aws337 Brain 2013: 136; 577–592 | 577

BRAIN
A JOURNAL OF NEUROLOGY

CHOP regulates the p53–MDM2 axis and is required for neuronal survival after seizures

Tobias Engel,[1,2] Amaya Sanz-Rodgriguez,[1,2] Eva M. Jimenez-Mateos,[1,2] Caoimhin G. Concannon,[1,2] Alba Jimenez-Pacheco,[1,2] Catherine Moran,[1] Guillaume Mesuret,[1,2] Emilie Petit,[3] Norman Delanty,[4] Michael A. Farrell,[4] Donncha F. O'Brien,[4] Jochen H. M. Prehn,[1,2] Jose J. Lucas[5,6] and David C. Henshall[1,2]

1 Department of Physiology and Medical Physics, Royal College of Surgeons in Ireland, Dublin, 2, Ireland
2 Centre for the Study of Neurological Disorders, Royal College of Surgeons in Ireland, Dublin, 2, Ireland
3 Molecular and Cellular Therapeutics, Royal College of Surgeons in Ireland, Dublin, 2, Ireland
4 Beaumont Hospital, Dublin, 9, Ireland
5 Center for Molecular Biology 'Severo Ochoa' (CBMSO), CSIC/UAM, Madrid, Spain
6 Networking Research Center on Neurodegenerative Diseases (CIBERNED), Instituto de Salud Carlos III, Madrid, Spain

Correspondence to: David C. Henshall,
Department of Physiology and Medical Physics,
Royal College of Surgeons in Ireland,
123 St. Stephen's Green,
Dublin 2, Ireland
E-mail: dhenshall@rcsi.ie

Hippocampal sclerosis is a frequent pathological finding in patients with temporal lobe epilepsy and can be caused by prolonged single or repeated brief seizures. Both DNA damage and endoplasmic reticulum stress have been implicated as underlying molecular mechanisms in seizure-induced brain injury. The CCAAT/enhancer-binding protein homologous protein (CHOP) is a transcriptional regulator induced downstream of DNA damage and endoplasmic reticulum stress, which can promote or inhibit apoptosis according to context. Recent work has proposed inhibition of CHOP as a suitable neuroprotective strategy. Here, we show that transcript and protein levels of CHOP increase in surviving subfields of the hippocampus after prolonged seizures (status epilepticus) in mouse models. CHOP was also elevated in the hippocampus from epileptic mice and patients with pharmacoresistant epilepsy. The hippocampus of *CHOP*-deficient mice was much more vulnerable to damage in mouse models of status epilepticus. Moreover, compared with wild-type animals, *CHOP*-deficient mice subject to status epilepticus developed more spontaneous seizures, displayed protracted hippocampal neurodegeneration and a deficit in a hippocampus-dependent object–place recognition task. The absence of CHOP was associated with a supra-maximal induction of p53 after status epilepticus, and inhibition of p53 abolished the cell death-promoting consequences of *CHOP* deficiency. The protective effect of CHOP could be partly explained by activating transcription of murine double minute 2 that targets p53 for degradation. These data demonstrate that CHOP is required for neuronal survival after seizures and caution against inhibition of CHOP as a neuroprotective strategy where excitotoxicity is an underlying pathomechanism.

Keywords: apoptosis; C/EBP homologous protein; DNA damage; epileptogenesis; hippocampal sclerosis; p53

Abbreviation: CA = cornu ammonis; CHOP = CCAAT/enhancer-binding protein homologous protein

Received July 23, 2012. Revised October 5, 2012. Accepted November 4, 2012. Advance Access publication January 29, 2013

Introduction

Epilepsy is a common, chronic neurological disorder characterized by recurrent, unprovoked seizures that are the result of abnormally synchronized neuronal discharges in the brain (Chang and Lowenstein, 2003). The aetiology of temporal lobe epilepsy, the most common and refractory syndrome in adults, is often unknown, but hippocampal sclerosis, comprising selective neuron loss with attendant gliosis, is present in about two-thirds of patients. Hippocampal sclerosis may be both cause and consequence of seizures, and recurring seizures contribute to progressive damage and cognitive impairments (Falconer, 1974; Kotloski *et al*., 2002; Mathern *et al*., 2002; Bernasconi and Bernhardt, 2010).

Preventing hippocampal damage is a potential therapeutic strategy for mitigation or prevention of epilepsy (Falconer, 1974; Fujikawa, 2006; Acharya *et al*., 2008; Sloviter, 2011). The pathomechanisms underlying seizure-induced neuronal death, however, are not fully understood. Prolonged glutamate receptor activation during a seizure leads to the loss of intracellular calcium homeostasis, oxidative stress, DNA damage and intracellular organelle dysfunction (Fujikawa, 2006). A biochemical signature consistent with neuronal apoptosis is also present, and targeting these pathways offers novel approaches for preventing hippocampal damage and post-injury spontaneous seizures (Henshall and Murphy, 2008; Engel *et al*., 2011).

The endoplasmic reticulum performs several functions, including protein folding and trafficking and regulating intracellular calcium levels (Xu *et al*., 2005). Seizure activity results in the activation of an endoplasmic reticulum stress response (Pelletier *et al*., 1999; Kitao *et al*., 2001; Yamamoto *et al*., 2006; Sokka *et al*., 2007). Endoplasmic reticulum stress is normally sensed by three upstream signalling proteins; the kinases PERK [protein kinase RNA (PKR)-like ER (endoplasmic reticulum) kinase] and IRE1 (inositol-requiring protein 1) and the transcription factor ATF6 (activating transcription factor 6). Together, these initiate the unfolded protein response that functions to upregulate endoplasmic reticulum chaperones, such as glucose-regulated protein 78, inhibit most protein translation and activate proteases involved in the degradation of misfolded proteins (Xu *et al*., 2005; Hetz, 2012). Prolonged endoplasmic reticulum stress, as well as DNA damage, can induce apoptosis through CCAAT/enhancer-binding protein homologous protein (CHOP) (Zinszner *et al*., 1998; Oyadomari and Mori, 2004; Tabas and Ron, 2011). CHOP is a member of the CCAAT/enhancer-binding protein family of transcription factors and can be induced by all three unfolded protein response arms, although the PERK–Eukaryotic initiation factor 2-α (eIF2α)–ATF4 pathway is essential (Szegezdi *et al*., 2006). CHOP functions mainly as a dominant-negative regulator of gene expression (Ron and Habener, 1992; Jauhiainen *et al*., 2012). The mechanism by which CHOP induces apoptosis involves repression of anti-apoptotic genes and induction of pro-apoptotic genes, among them the B-cell lymphoma 2 (Bcl-2) Bcl-2 homology domain 3-only proteins Bcl-2 interacting mediator of death (Bim) (Puthalakath *et al*., 2007; Ghosh *et al*., 2012) and p53 upregulated mediator of apoptosis (Puma) (Galehdar *et al*., 2010; Ghosh *et al*., 2012).

CHOP has been reported to promote neuronal death in models of neurodegeneration (Milhavet *et al*., 2002; Reijonen *et al*., 2008; Chigurupati *et al*., 2009; Prasanthi *et al*., 2011) and after acute brain insults (Tajiri *et al*., 2004; Cui *et al*., 2007; He *et al*., 2012), and, reasonably, CHOP inhibition has been proposed as a neuroprotective strategy. Recent studies, however, showed that CHOP can be anti-apoptotic, promoting neuronal survival after endoplasmic reticulum stress, hypoxia and protecting against oligodendrocyte death (Gow and Wrabetz, 2009; Halterman *et al*., 2010; Rouschop *et al*., 2010; Chen *et al*., 2012). Although CHOP has been reported to be induced after seizures (Murphy *et al*., 2010; Chihara *et al*., 2011), no functional studies have been undertaken. We, therefore, investigated the role of CHOP in seizure-induced neuronal death in experimental and human epilepsy.

Materials and methods

Mouse seizure models

All animal experiments were performed in accordance with the principles of the European Communities Council Directive (86/609/EEC), and procedures were approved by the Research Ethics Committee of the Royal College of Surgeons in Ireland. Adult C57BL/6 wild-type (Harlan), *Chop*$^{+/-}$ and *Chop*$^{-/-}$, mice (Jackson Laboratory; B6.129S-*Ddit3*^{tm1Dron}/J; Zinszner *et al*., 1998) were used. *Chop*$^{-/-}$ mice were originally back-crossed to C57BL/6 background for at least five generations and were, subsequently, further back-crossed. Mice were anaesthetized and placed in a stereotaxic frame. Three partial craniectomies were performed to affix cortical skull-mounted EEG electrodes (Plastics One), and EEG was recorded using a Grass Comet digital EEG. A guide cannula was affixed for intra-amygdala targeting, and the skull assembly was fixed in place with dental cement. After baseline EEG, kainic acid (0.3 μg in 0.2 μl PBS) (Ocean Produce International) was microinjected into the basolateral amygdala. Non-seizure control mice received 0.2 μl of intra-amygdala vehicle. Forty minutes later, mice received intraperitoneal lorazepam (6 mg/kg).

Seizure preconditioning was induced by a single intraperitoneal injection of kainic acid (15 mg/kg in 0.2 ml PBS) (Hatazaki *et al*., 2007). Sham-preconditioned animals received the same volume of PBS. To model epileptic tolerance, status epilepticus was induced after preconditioning by intra-amygdala microinjection of kainic acid (0.3 μg in 0.2 μl PBS). A group of sham-preconditioned mice also underwent status epilepticus induced by intra-amygdala kainic acid and served as injury control subjects. Lorazepam (6 mg/kg, intraperitoneal) was administered to all animals 40 min after intra-amygdala injections. In additional mice, status epilepticus was induced by subcutaneous injection of pilocarpine (Sigma-Aldrich) at 340 mg/kg body weight, 20 min after injection of methyl-scopolamine (1 mg/kg) (Sigma-Aldrich).

Mice were saline-perfused under deep anaesthesia to remove intravascular blood components, and brains were either flash-frozen whole in 2-methylbutane at 30°C for histopathology, perfused with 4% paraformaldehye for immunofluorescence and *in situ* hybridization, dissected on ice to obtain whole hippocampus and cortex or microdissected to obtain the different hippocampal subfields [cornu ammonis (CA)1, dentate gyrus and CA3].

Salubrinal, tunicamycin and pifithrin-α treatment

Mice received a 2 μl intracerebroventricular injection of 75 μM salubrinal (Calbiochem) or 5 μmol tunicamycin (Sigma-Aldrich) 4 or 8 h

before intra-amygdala kainic acid, respectively. Vehicle mice received dimethyl sulphoxide alone. For p53 inhibitor studies, wild-type and *Chop*$^{-/-}$ mice received intraperitoneal vehicle (0.1% dimethyl sulphoxide in PBS) or pifithrin-α [1-(4-methylphenyl)-2-(4,5,6,7-tetrahydro-2-imino-3(2H)-benzothiazolyl)-ethanone hydrobromide] (Sigma-Aldrich) at 4 mg/kg as described previously (Engel *et al*., 2010*a*). Pifithrin-α was administered 24 h before, 1 h after status epilepticus and on the first and second day after status epilepticus.

Quantification of electroencephalography

Digitized EEG recordings were analysed off-line using manual assessment and automated software as described (Engel *et al*., 2012). The duration of high-frequency (>5 Hz) and high-amplitude (>2 times baseline) polyspike discharges of ⩾5 s duration, which are synonymous with injury-causing electrographic activity, was counted by a reviewer blind to the treatment. Further EEG analysis was performed by uploading EEG into Labchart7 software (ADInstruments) to calculate amplitude of the EEG signal.

Epilepsy monitoring

Continuous EEG recordings were performed using implantable EEG telemetry units (Data Systems International) (Engel *et al*., 2010*a*, *b*). Transmitters (model F20-EET, Data Sciences International) were implanted in a subcutaneous pocket and were used to record bilateral EEG from skull. EEG data were acquired beginning on the third day after status epilepticus until day 14. Seizures were defined as high frequency (>5 Hz), high amplitude (>2 times baseline) polyspike discharges of ⩾5 s duration. Additional epilepsy monitoring was performed 4 weeks post-status epilepticus by continuous video-only monitoring of generalized tonic–clonic seizures, as described (Jimenez-Mateos *et al*., 2012).

Object location memory task

Object location memory experiments were performed as described previously (Wimmer *et al*., 2012) with minor modifications. On the training day, mice were placed in a training arena consisting of a 30 × 30 × 20 cm box with transparent walls, for four 10-min sessions with an inter-session interval of 3 min, during which mice were returned to their home cages. The first session consisted of a context habituation period without objects in the arena. During the next three sessions, mice were placed in the training arena with two distinct objects. The objects and the arenas were wiped with 70% ethanol before each session. Twenty-four hours after training, mice were placed in the original training arena for 10 min with one object displaced to a new location, whereas the other object was not moved. Exploration was recorded during training and testing on a digital camera for subsequent scoring of time spent exploring objects. Total distance travelled, velocity and time spent in the demarcated central zone of the arena were automatically analysed using Ethovision videotracking (Ethovision). Exploration of objects was measured manually by stopwatch and was defined as the amount of time mice were oriented towards an object with its nose within 1 cm of it, and it was scored by an experimenter blinded to treatment and genotype.

Human brain tissue samples

This study was approved by the Ethics (Medical Research) Committee of Beaumont Hospital, Dublin (05/18), and written informed consent was obtained from all patients. Briefly, control (autopsy) hippocampus ($n = 4$; C1–C4) and temporal cortex ($n = 5$; C5–C9) were obtained from five individuals from the Brain and Tissue Bank for Developmental Disorders at the University of Maryland, Baltimore, MD, USA. Patients ($n = 12$) were referred for surgical resection of the temporal lobe for the treatment of intractable temporal lobe epilepsy. After temporal lobe resection, the hippocampus and/or neocortex was obtained and frozen in liquid nitrogen and was stored at −70°C until use. A pathologist (M.F.) assessed hippocampus ($n = 9$) and neocortex ($n = 3$) and described the presence of hippocampal sclerosis and other pathological changes. Samples were then processed for protein analysis by western blot. Full details of control and patient pathology and clinical data can be found elsewhere (McKiernan *et al*., 2012).

RNA extraction and real-time quantitative polymerase chain reaction

RNA extraction was undertaken as previously described using TRIzol® (Invitrogen) (Hatazaki *et al*., 2007). Briefly, 1 μg of total RNA was used to generate complementary DNA by reverse transcription using SuperScript® II reverse transcriptase enzyme (Invitrogen). Quantitative real-time PCR was performed using a LightCycler 1.5 (Roche Diagnostics) in combination with QuantiTect® SYBR® Green PCR kit (Qiagen) as per manufacturer's protocol, and 1.25 μM of primer pair was used. Data were analysed by LightCycler 1.5 software, data were normalized to expression of β-actin and represented as relative quantification values. Primers were designed using Primer3 software (http://frodo.wi.mit.edu) and were verified by basic local alignment search tool BLAST (http://blast.ncbi.nlm.nih.gov/Blast.cgi). Primers sequences: *Arc*: forward 5′-TGACTCACAACTGCCACACA-3′, reverse-5′-ATGAGGAAGCCAGATCGTGT-3′; *Chop*: forward 5′-GAATAACAGCCGGAACCTGA-3′, reverse 5′-CGTTTCCTGGGGATGAGATA-3′; WAF; wild-type p53-activated fragment; Cip1; Cdk interacting protein 1; $p21^{WAF/Cip1}$: forward 5′-CCGTGGACAGTGAGCAGTTG-3′, reverse 5′-GCAGCAGGGCAGAGGAAGTA-3′; *p53*: forward 5′-CGGGTGGAAGGAAATTTGTA-3′, reverse 5′-GCACAAACACGAACCTCAAA-3′; *Mdm2*: forward 5′-GAAATGAATCCTCCCCTTCC-3′, reverse 5′-CTGTCAGCTTTTTGCCATCA-3′; spliced *Xbp1*: forward 5′-GAGTCCGCAGCAGGTG-3′, reverse 5′-AAGGGAGGCTGGTAAGGAA-3′.

Microarray analysis

Microarray studies were undertaken according to previously described techniques (Hatazaki *et al*., 2007) at an Affymetrix authorized service provider (University College Dublin, Dublin, Ireland). Briefly, total RNA was extracted from control wild-type mice and wild-type and *Chop*$^{-/-}$ mice 6 h after status epilepticus and was hybridized to the Mouse Genome 430 2.0 Genechip array. Affymetrix GeneChip image files were analysed by robust multichip analysis using RMAExpress 0.5 (http://rmaexpress.bmbolstad.com). Data were log transformed, and the threshold for significant regulation was set at 2-fold to retain genes that exhibit a biologically meaningful level of regulation, but not exclude certain genes that, because of high constitutive expression, may show lower degrees of change. Gene ontology and function were assigned by interrogating the database for annotation, visualization and integrated discovery (http://david.abcc.ncifcrf.gov/) and the published literature.

In situ hybridization

The probe to detect *Chop* was 5′-digoxigenin-labelled, 2-*O*,4-*C*-methylene bicyclonucleoside monomer containing oligonucleotide. The sequence was the reverse complement to the mature *Chop* messenger RNA; /5DigN/GGCCATAGAACTCTGACTGGAA (Exiqon). Probes were incubated 1:200 in hybridization buffer overnight at 60°C. On the next day, anti-digoxigenin-alkaline phosphatase antibody (1:1000; Roche) was incubated, and on the following day, sections were washed, and colour substrate solution (Roche) was added to each slide until signal appeared.

Western blot analysis

Western blotting was performed as previously described (Engel *et al*., 2010*a*). Proteins were extracted from hippocampus, separated by SDS–PAGE and transferred to nitrocellulose membranes and then immunoblotted with the following primary antibodies: ATF-4, ATF-6α, CHOP, MDM2 and p53 (Santa Cruz Biotechnology); eIF2α, Phospho-eIF2α (Ser51) and Lamin A/C (Cell Signaling Technology); GluR6/7 (Millipore); KDEL (Assay Designs); PUMA (ProSci Inc.) and β-actin and α-tubulin (Sigma-Aldrich). Horseradish peroxidase-conjugated antibodies (Cell Signaling Technology) were then applied and used as secondary antibodies. Protein bands were visualized using SuperSignal® West Pico Chemiluminescent Substrate (Pierce). Gel band image densities were captured using a Fuji-film LAS-3000 and analysed using Alpha-EaseFC4.0 software.

DNA damage assessment

A competitive ELISA (Cambridge Bioscience) was used for the quantitative measurement of 8-hydroxydeoxyguanosine. Samples with unknown 8-hydroxydeoxyguanosine content and standards were first added to an 8-hydroxydeoxyguanosine/bovine serum albumin conjugate plate and incubated for 10 min at room temperature. Anti-8-hydroxydeoxyguanosine monoclonal antibody was added and incubated for 1 h at room temperature, followed by incubation with the horseradish peroxide-conjugated secondary antibody for 1 h. The 8-hydroxydeoxyguanosine content in samples was determined by comparison with the predetermined 8-hydroxydeoxyguanosine standard curve.

Histopathology

Fresh-frozen coronal brain sections at the level of the dorsal and ventral hippocampus were air-dried, fixed in formalin and stained with antibodies against NeuN (Chemicon) and detected by goat anti-mouse Alexa Fluor® 568 (BioSciences Ltd). Neuronal damage was assessed by Fluoro-Jade B staining (Millipore) (Engel *et al*., 2010*a*). Analysis of DNA damage was performed using a fluorescein-based terminal deoxynucleotidyl dUTP nick end-labelling technique (Promega). Sections were mounted in medium containing 4,6 diamidino-2-phenylindole (DAPI; Vector Laboratories) to visualize nuclei. Sections were imaged using a Nikon 2000s epifluorescence microscope with a Hamamatsu Orca 285 camera (Micron-Optical). Semi-quantification of damaged and/or surviving cell numbers was performed for the entire CA3 subfield, beginning at the border with CA2 through to the end of CA3c/CA4 within the hilus of the dentate gyrus and for the entire CA1 subfield beginning at border with CA2 through to the end of CA1. For area measurements of the dentate gyrus, sections were stained with DAPI and delineated using MetaMorph. Next, DAPI-positive cells in the delineated area were counted with ImageJ, and area was divided by total count of DAPI positive cells. Counts were the average of two adjacent sections assessed by an observer masked to experimental group/condition.

Confocal microscopy

For confocal microscopy, animals were transcardially perfused with 4% paraformaldehyde, post-fixed and cryoprotected in sucrose before sectioning. Sections were rinsed and treated with PBS containing 0.1% Triton™ X-100 and 1% foetal calf serum followed by incubation with the primary antibodies; p53 (Novocastra) and cleaved caspase 3 (Cell Signaling Technology). Sections were washed again and incubated with secondary antibodies coupled to Alexa Fluor® 488 or Alexa Fluor® 568 (BioSciences Ltd). Sections were then coverslipped with Fluorosave™. Confocal images were acquired with a Leica TCR 6500 microscope equipped with four laser lines (405, 488, 561 and 653 nm) using a ×63 immersion oil objective.

Diaminobenzidine staining

Mice were perfused with 4% paraformaldehyde, brains extracted, post-fixed and cryoprotected in 30% sucrose solution, and 30-µm sagittal sections were cut on a Leica cryostat. Next, brain sections were pretreated for 1 h with 1% bovine serum albumin, 5% foetal bovine serum and 0.2% Triton™ X-100 and then incubated with p53 (Novocastra) primary antibody. Finally, brain sections were incubated in avidin–biotin complex using the Elite® VECTASTAIN® kit (Vector Laboratories). Chromogen reactions were performed with diaminobenzidine (Sigma-Aldrich) and 0.003% hydrogen peroxide for 10 min. Sections were coverslipped with Fluorosave™.

Plasmids and luciferase reporter experiments

The putative *Mdm2* promoter was cloned by PCR amplification from mouse genomic DNA of a fragment containing the region −1923 to +193 relative to the transcription initiation site and cloned into the SacI and HindIII sites of the pGL3-Basic vector (Promega). The CHOP expression plasmid was similarly cloned by PCR amplification of mouse complementary DNA and cloned into the pIRES2-EGFP biscistronic vector (Clontech). The integrity of all constructs was verified by sequencing. SHSY5y cells were transfected with the MDM2–pGL3 plasmid along with the Renilla Luciferase expressing plasmid, phRL-TK-luc (Promega) and the plasmid expressing CHOP or the empty vector control using Metafectene® (Biontex) as per the manufacturer's instructions. After 24 h, cells were lysed in passive lysis buffer (Promega), and luciferase activity was measured using the Dual Luciferase Reporter Assay System (Promega), and the resulting luminescence was monitored using a Berthold luminometer. Luminescence was calculated as a ratio of Firefly/Renilla activity and expressed relative to control transfected wells.

Simulated post-mortem delay

Hippocampi were extracted from mice (adult C57Bl/6) after deep anaesthesia with pentobarbital and decapitation. Hippocampi were either frozen immediately ('surgical' control) or frozen 4 or 8 h after being left at room temperature (simulated post-mortem interval). Samples were then processed for western blotting as described earlier in the text.

Data analysis

Data are presented as means ± standard error of the mean (SEM). Data were analysed using ANOVA with *post hoc* Fisher's protected least significant difference test, Student's *t*-test for two-group comparison and Mann–Whitney test for non-parametric test (StatView). Significance was accepted at $P < 0.05$.

Results

CHOP is upregulated in surviving regions of the hippocampus after status epilepticus

We first examined CHOP in a well-characterized model of status epilepticus produced by intra-amygdala microinjection of the glutamate receptor agonist kainic acid in mice (Engel *et al*., 2010*a*; Murphy *et al*., 2010). Status epilepticus caused damage to the ipsilateral CA3 subfield, whereas neurons in the CA1 subfield and dentate gyrus were largely spared (Fig. 1A). Analysis of lysates from whole hippocampus determined all three branches of the unfolded protein response were activated after status epilepticus, with increased eIF2α phosphorylation and ATF4 protein levels, increased ATF6 cleavage and *Xbp1* splicing (Fig. 1B–D). Increased levels of *Chop* messenger RNA (Fig. 1E) and CHOP protein (Fig. 1F and G) were detected by 8 h. CHOP protein also increased in the nucleus after status epilepticus (Fig 1H), which may be important for CHOP to execute its transcriptional functions (Jauhiainen *et al*., 2012). CHOP induction after seizures was not unique to this kainic acid model and occurred at both transcript and protein level after status epilepticus induced by the cholinergic agonist pilocarpine (Fig. 1I–K).

To determine whether CHOP induction was restricted to damaged parts of the hippocampus, we measured transcript levels in microdissected CA3, CA1 and the dentate gyrus. Surprisingly, *Chop* messenger RNA was induced in non-damaged (CA1, dentate gyrus) as well as damaged (CA3) subfields (Fig. 2A). Western blot analysis confirmed CHOP protein increased in each subfield (Supplementary Fig. 1A). *In situ* hybridization also showed *Chop* messenger RNA was present in neurons in each subfield (Supplementary Fig. 1B).

CHOP upregulation in response to neuroprotective manipulations *in vivo*

To investigate whether CHOP was associated with neuronal survival in other contexts, we subjected additional mice to a single episode of brief generalized seizure activity produced by intraperitoneal injection of 15 mg/kg kainic acid. These seizures do not damage the hippocampus, and instead, they activate endogenous programmes of neuroprotection that protect against status epilepticus (Hatazaki *et al*., 2007). CHOP protein was increased in all three major subfields of the hippocampus after seizure preconditioning (Fig. 2B). We also treated mice with the endoplasmic reticulum stress inhibitor salubrinal, which blocks eIF2α phosphorylation and has been reported to protect against seizure-induced neuronal death *in vivo* (Sokka *et al*., 2007; Moon *et al*., 2011). An intracerebroventricular injection of salubrinal increased CHOP protein in the mouse hippocampus (Fig. 2C) and decreased neuronal death after intra-amygdala kainic acid-induced seizures (Fig. 2D and E).

Normal hippocampal architecture and response to kainic acid in *Chop*$^{-/-}$ mice

If CHOP is functioning to prevent rather than promote seizure-induced neuronal death, then loss of CHOP should increase seizure damage. To test this idea, we studied mice lacking CHOP (*Chop*$^{-/-}$) (Zinszner *et al*., 1998). CHOP-deficient mice were born at expected rates, developed normally and displayed no abnormal brain morphology. Coronal brain sections stained for the neuronal marker NeuN confirmed normal hippocampal architecture (Supplementary Fig. 2A and B). No differences were observed between wild-type and *Chop*$^{-/-}$ mice for basal levels of the kainate receptor GluR6/7 (Supplementary Fig. 2D and E). We then equipped mice with skull-mounted electrodes and recorded EEG after inducing status epilepticus by intra-amygdala kainic acid. Levels of the activity-regulated gene *Arc* were increased to the same level in wild-type and *Chop*$^{-/-}$ mice subject to status epilepticus (Supplementary Fig. 2F). No differences were observed between wild-type, *Chop*$^{+/-}$ and *Chop*$^{-/-}$ animals in total seizure time, EEG amplitude or frequency (Supplementary Fig. 2G–I). Seizure-induced DNA damage was also similar between *Chop*$^{-/-}$ mice and wild-type animals (Supplementary Fig. 3).

Increased hippocampal damage in *Chop*$^{-/-}$ mice after status epilepticus

We next examined seizure-induced neuronal death 72 h after status epilepticus in wild-type, *Chop*$^{+/-}$ and *Chop*$^{-/-}$ mice (Fig. 3). Mice lacking CHOP displayed more damage to the CA3 subfield compared with heterozygous and wild-type littermates (Fig. 3A and Supplementary Fig. 4A). Extensive neuronal death was also present in hippocampal subfields of *Chop*$^{-/-}$ mice that do not normally undergo seizure-induced neuronal death in this model, including the CA1 and dentate gyrus (Fig. 3B and C and Supplementary Fig. 4B and C). Increased damage in *Chop*$^{-/-}$ mice was also found in the ventral hippocampus (Supplementary Fig. 5). The difference in damage was also present in *Chop*$^{-/-}$ mice killed 24 h after status epilepticus (Supplementary Fig. 6). Mice lacking *CHOP* also displayed increased seizure-induced neuronal death in response to pilocarpine-induced status epilepticus (Fig. 3D). We also examined the contralateral hippocampus of mice, as this is another area normally undamaged in the model (Mouri *et al*., 2008). Western blot analysis determined CHOP was strongly upregulated in the contralateral hippocampus (Supplementary Fig. 7A and B) and histopathology revealed extensive neurodegeneration in the contralateral hippocampus of *Chop*$^{-/-}$ mice but not wild-type animals after status epilepticus (Supplementary Fig. 7C–F).

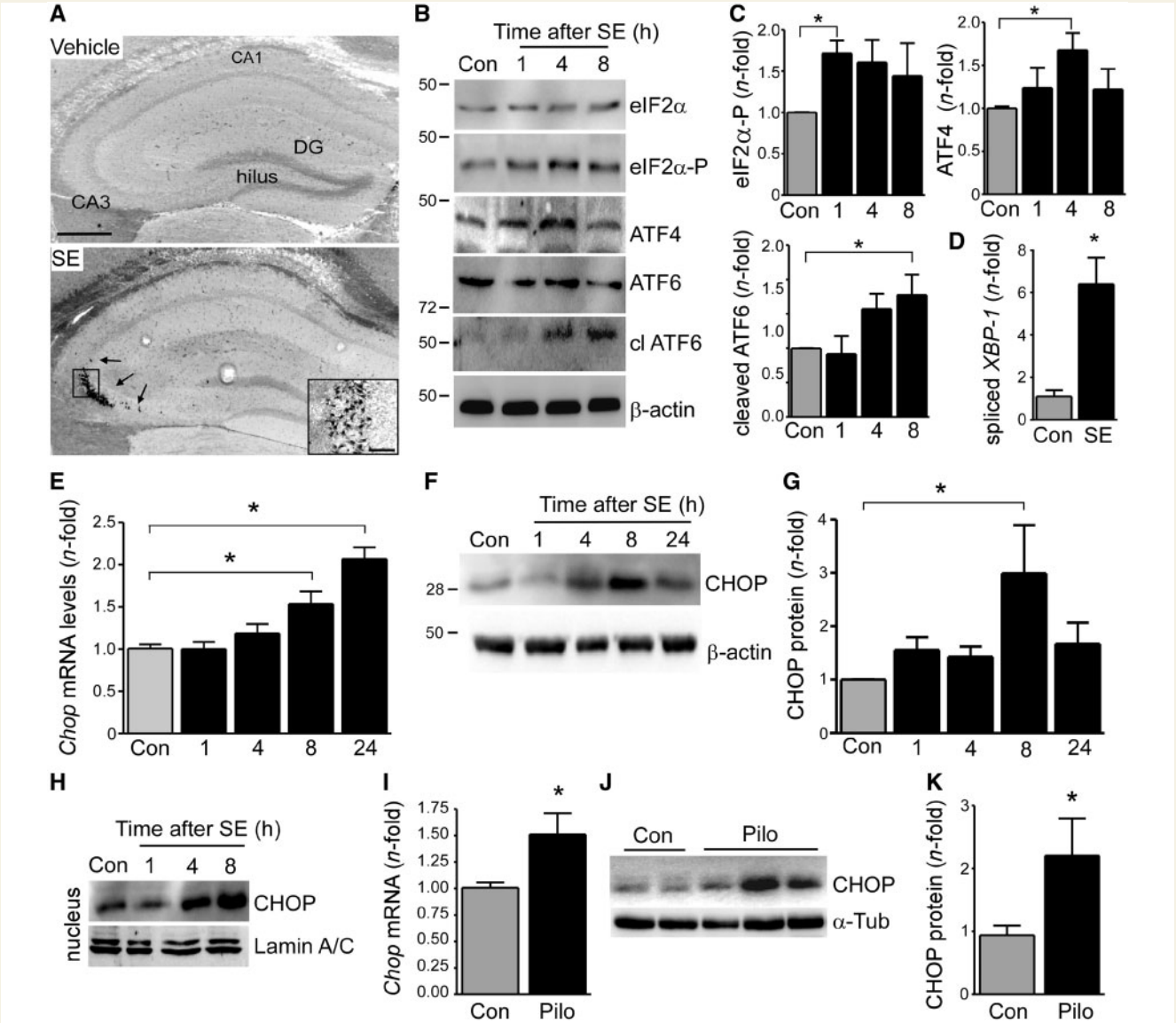

Figure 1 Status epilepticus upregulates CHOP in mouse models. (**A**) Representative photomicrographs showing Fluoro-Jade B staining (arrows) 24 h after status epilepticus (SE) in the CA3 subfield, whereas CA1 and dentate gyrus (DG) regions are largely spared. Inset shows higher magnification view of Fluoro-Jade B-positive cells in CA3. (**B**) Representative western blots ($n = 1$ per lane) from whole hippocampus showing increased eIF2α phosphorylation (P), ATF4 protein levels and ATF6 splicing after status epilepticus. (**C**) Increased phosphorylation of eIF2α, higher ATF4 protein levels and ATF6 splicing after status epilepticus in whole hippocampal cell lysates ($n = 4$–7/group). (**D**) Graph showing spliced *Xbp1* (s*Xbp-1*) levels 6 h after status epilepticus ($n = 4$–7/group). (**E**) *Chop* messenger RNA levels in whole hippocampus after status epilepticus ($n = 4$–6/group). (**F** and **G**) Western blot ($n = 1$ per lane) and graph showing CHOP in whole hippocampus after status epilepticus ($n = 6$–7/group). (**H**) Western blot ($n = 3$ per lane) showing nuclear CHOP after status epilepticus. (**I**) Increased *Chop* messenger RNA levels in hippocampus 4 h after pilocarpine (Pilo)-induced seizures ($n = 8$–10/group). (**J** and **K**) Western blot ($n = 1$ per lane) and graph showing CHOP protein in hippocampus 4 h after pilocarpine-induced seizures ($n = 4$–6/group). Con = control; statistically significant differences are indicated by $^*P < 0.05$. Data presented as mean ± SEM. Scale bar = 250 μm.

Neuroprotection by endoplasmic reticulum stress preconditioning is lost in *Chop*$^{-/-}$ mice

We next examined seizure damage in wild-type and *Chop*$^{-/-}$ mice previously exposed to mild endoplasmic reticulum stress. Mice were given an intracerebroventricular injection of tunicamycin 8 h before status epilepticus at a dose that increased CHOP and endoplasmic reticulum stress (Supplementary Fig. 8) but did not cause cell death. In wild-type mice, the endoplasmic reticulum stress preconditioning protected against seizure-induced neuronal death (Fig. 3E). In contrast, seizure-induced neuronal death was exacerbated by endoplasmic reticulum stress preconditioning in *Chop*$^{-/-}$ mice (Fig. 3E).

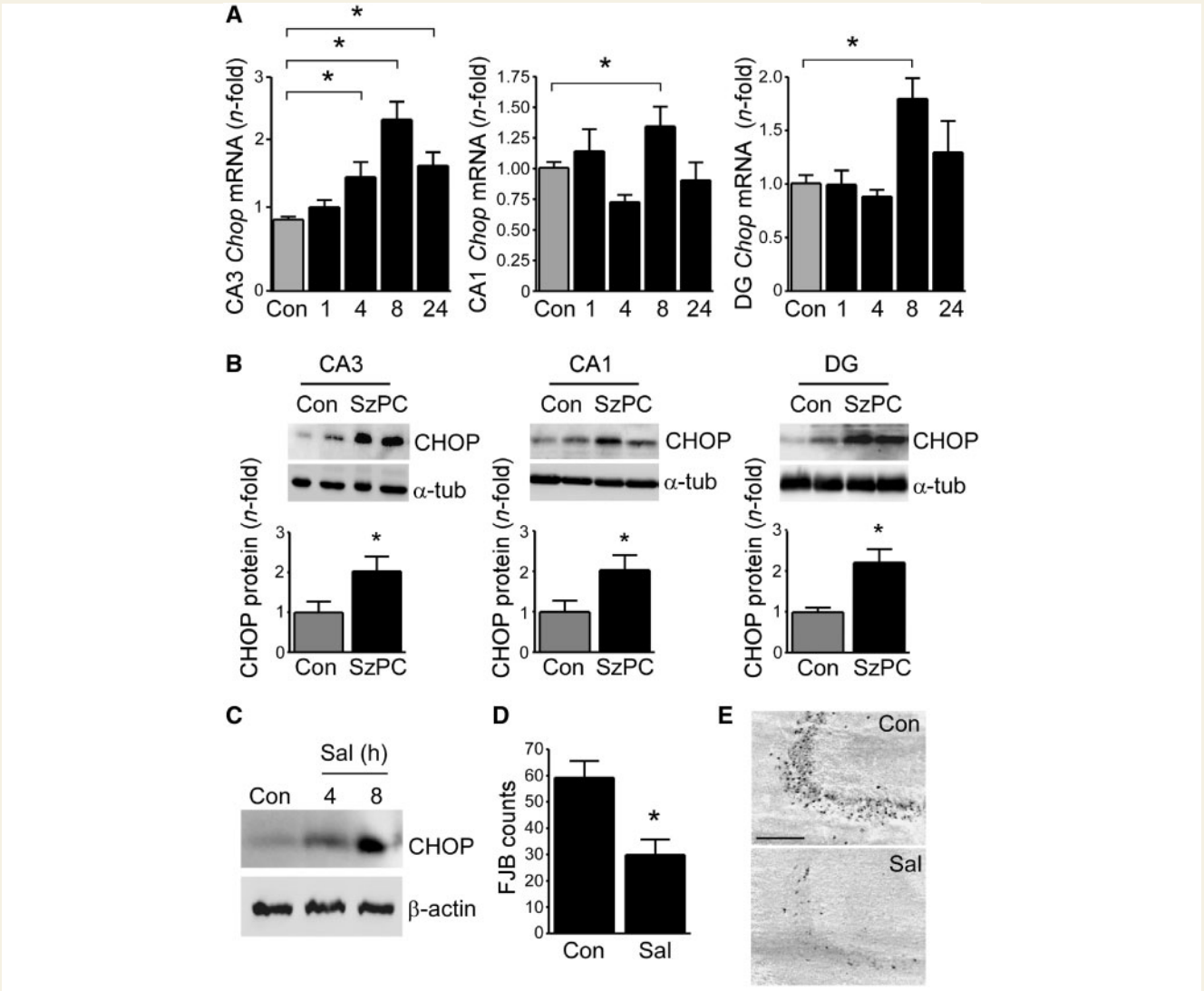

Figure 2 CHOP upregulation in damage-resistant subfields after status epilepticus. (**A**) Real-time PCR analysis of *Chop* messenger RNA levels in CA3, CA1 and dentate gyrus (DG) after status epilepticus ($n = 4$/group). (**B**) Graphs and (above) representative blots ($n = 1$ per lane) showing CHOP levels in the different hippocampal subfields 24 h after seizure preconditioning (SzPC) ($n = 6$/group). (**C**) Western blot ($n = 1$ per lane) showing CHOP protein 4 and 8 h after injection of 75 μM salubrinal (Sal). (**D**) Graph showing reduced Fluoro-Jade B (FJB) counts in the CA3 subfield 24 h after status epilepticus in mice pretreated with salubrinal compared with vehicle control subjects ($n = 10$/group). (**E**) Representative photomicrographs of Fluoro-Jade B staining in the CA3 subfield at 24 h. Statistically significant differences are indicated by $^*P < 0.05$. Scale bar = 150 μm. Data presented as mean ± SEM.

Increased p53 levels after status epilepticus in the absence of CHOP

The mechanism by which CHOP regulates cell death is thought to involve inducing or curtailing expression of a subset of apoptosis-associated genes (Oyadomari and Mori, 2004; Jauhiainen *et al.*, 2012). To identify which genes might be dysregulated in $Chop^{-/-}$ mice, we profiled gene expression in wild-type and $Chop^{-/-}$ mice after status epilepticus using microarrays (Hatazaki *et al.*, 2007). Overall, status epilepticus resulted in similar numbers and fold changes of gene expression between wild-type and $Chop^{-/-}$ mice (Fig. 4A–C). However, the number of genes involved in the regulation of cell death and the p53 pathway was higher in $Chop^{-/-}$ mice compared with wild-type animals (Fig. 4D). In particular, expression of multiple p53-regulated genes was increased in $Chop^{-/-}$ mice (Fig. 4E).

To confirm that an absence of CHOP resulted in higher p53 activity, we measured the expression of $p21^{WAF/Cip1}$ after status epilepticus, a marker of p53 activity in this model (Engel *et al.*, 2010*a*). $p21^{WAF/Cip1}$ levels after status epilepticus were higher in $Chop^{-/-}$ mice compared with wild-type animals (Fig. 4F). Protein levels of p53, but not messenger RNA, were higher in $Chop^{-/-}$ mice after status epilepticus compared with wild-type animals (Fig. 4G–J). There was no basal difference in p53 protein levels between $Chop^{-/-}$ mice and wild-type animals (Fig. 4J and K). Analysis of the temporal relationship between p53 and neuronal

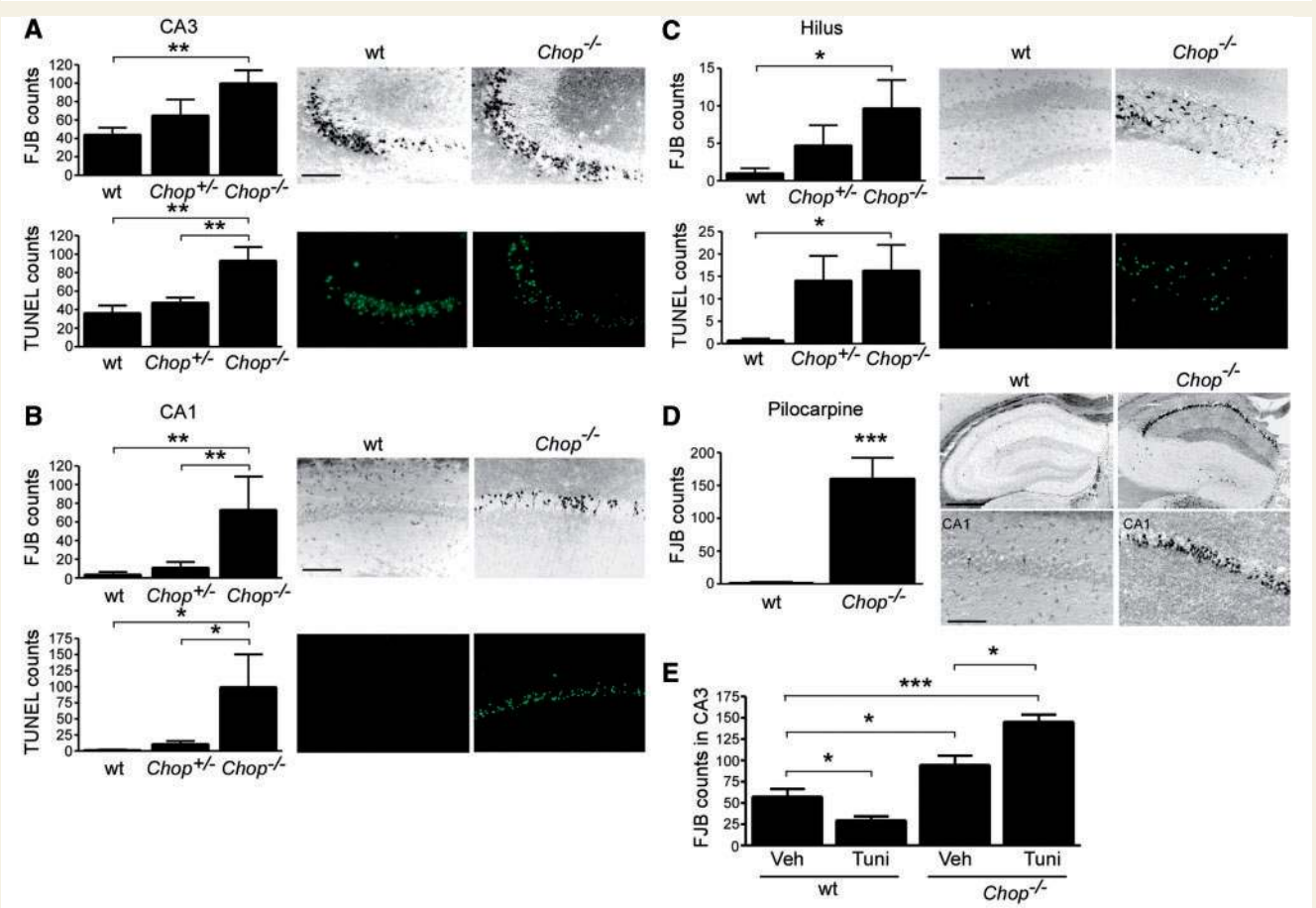

Figure 3 Increased hippocampal damage in *Chop*$^{-/-}$ mice after status epilepticus. (**A–C**) Graphs and representative photomicrographs showing Fluoro-Jade B and DNA damage (TUNEL) staining in (**A**) CA3, (**B**) CA1 and (**C**) hilus, of the ipsilateral hippocampus in *Chop*$^{-/-}$ mice compared with heterozygous and wild-type mice 72 h after intra-amygdala kainate-induced status epilepticus (n = 11–14/group). (**D**) Graph and photomicrographs (field view and CA1) showing cell death (Fluoro-Jade B staining) in *Chop*$^{-/-}$ mice 72 h after pilocarpine-induced status epilepticus compared with wild-type mice (n = 5/group). Note increased cell death in *Chop*$^{-/-}$ mice in the CA1 hippocampal subfield. (**E**) Graph showing Fluoro-Jade B counts 24 h after status epilepticus induced by intra-amygdala kainate in wild-type and *Chop*$^{-/-}$ mice given vehicle or a low dose of the endoplasmic reticulum stressor tunicamycin (Tuni) 8 h earlier. Statistically significant differences are indicated by $*P < 0.05$; $**P < 0.01$; $***P < 0.001$. Scale bar = 150 μm (**A–C** and **D** *lower panels*) and 250 μm (**D** *upper panels*). Data presented as mean ± SEM. FJB = Fluoro-Jade B; TUNEL = terminal deoxynucleotidyl transferase dUTP nick end labelling; veh = vehicle; wt = wild-type.

death showed p53 levels peaked ~4–24 h after status epilepticus, returning to baseline thereafter in wild-type mice, whereas p53 levels continued to increase over time in *Chop*$^{-/-}$ mice (Fig. 4J and K). Neuronal death also showed an increase between 24 and 72 h in *Chop*$^{-/-}$ mice but not in wild-type animals (Fig. 4L).

Inhibition of p53 in *Chop*$^{-/-}$ mice reduces seizure-induced neuronal death to wild-type levels

Immunohistochemistry confirmed high p53 levels in neurons in all major hippocampal subfields in *Chop*$^{-/-}$ mice that contrasted the p53 staining in wild-type animals after status epilepticus (Fig. 5A and B). Consistent with this promoting apoptosis, we observed more cleaved caspase 3 immunoreactivity in p53-positive CA3 neurons in *Chop*$^{-/-}$ mice compared with wild-type animals (Fig. 5C).

We previously reported that Puma is the effector of p53-induced neuronal death after status epilepticus (Engel *et al.*, 2010*a*). We found Puma protein levels were higher in the hippocampus of mice lacking *CHOP* after status epilepticus compared with wild-type animals (Fig. 5D and E).

If increased p53 levels are responsible for the enhanced seizure-induced neuronal death in *Chop*$^{-/-}$ mice, then p53 inhibition should prevent that injury. We tested this idea by treating mice with the p53 transcriptional inhibitor pifithrin-α (Engel *et al.*, 2010*a*). We confirmed pifithrin-α blocked p53 activity by assaying $p21^{WAF/Cip1}$ levels after status epilepticus (Fig. 5F) and found that the increased seizure-induced hippocampal damage in *Chop*$^{-/-}$ mice was prevented by pifithrin-α (Fig. 5G and H).

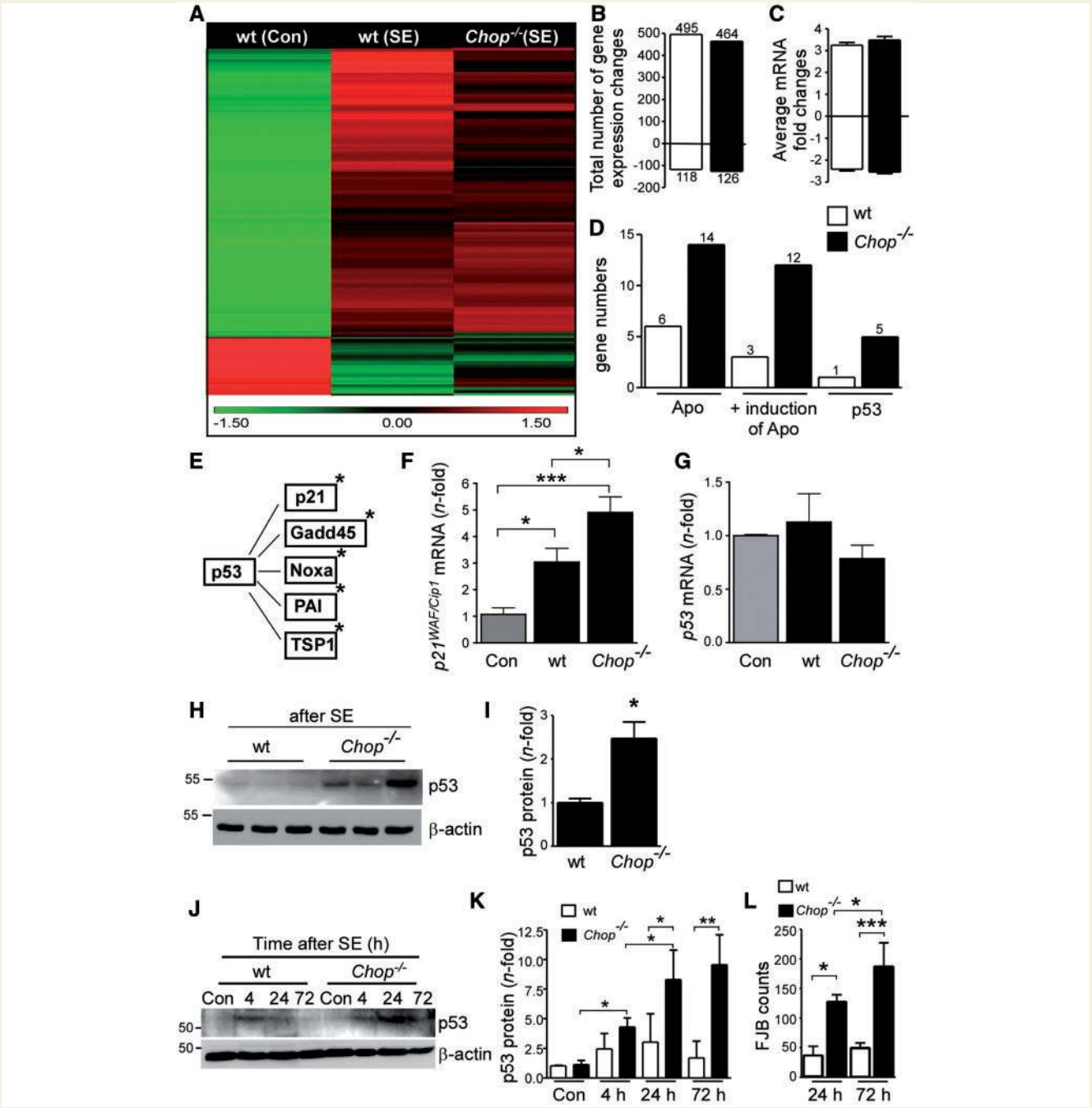

Figure 4 Increased p53 in *Chop*$^{-/-}$ mice after status epilepticus. (**A**) 'Heatmap' representing microarray analysis of the ipsilateral hippocampus 6 h after status epilepticus (SE) in wild-type (wt) and *Chop*$^{-/-}$ mice. (**B** and **C**) Microarray analysis found similar numbers and fold changes for genes up- and downregulated after status epilepticus between genotypes. (**D**) Graph showing number of genes involved in apoptosis (Apo), positive induction of Apo and in the p53 pathway with a fold increase >2 (compared with control wild-type) in wild-type or *Chop*$^{-/-}$ mice. (**E**) p53 target genes with higher fold increase (*) in *Chop*$^{-/-}$ mice when compared with wild-type mice after status epilepticus. (**F**) Hippocampal *p21*$^{WAF/Cip1}$ messenger RNA levels in wild-type and *Chop*$^{-/-}$ mice 6 h after status epilepticus when compared with control wild-type mice (n = 4–7/group). (**G**) Graph showing hippocampal *p53* messenger RNA levels after status epilepticus in wild-type and *Chop*$^{-/-}$ mice (n = 4–7/group). (**H** and **I**) Western blot and graph showing hippocampal p53 protein levels in *Chop*$^{-/-}$ mice compared with wild-type mice 6 h after status epilepticus (n = 3–4/group). (**J** and **K**) Western blot and densitometric analysis of p53 protein levels in *Chop*$^{-/-}$ mice 24 and 72 h after status epilepticus compared with seizure wild-type mice at same time points. No difference was observed in p53 protein levels between wild-type and *Chop*$^{-/-}$ control mice (n = 3/group). (**L**) Significantly more Fluoro-Jade B-positive cells in *Chop*$^{-/-}$ mice at 72 h after status epilepticus when compared with 24 h after status epilepticus. Similar levels of damage at both time-points can be observed in wild-type mice (n = 6–14/group). Statistically significant differences are indicated by $*P < 0.05$; $**P < 0.01$; $***P < 0.001$. Data presented as mean ± SEM. FJB = Fluoro-Jade B; SE = status epilepticus; wt = wild-type; Gadd45, Growth arrest and DNA damage 45; PAI, plasminogen activator inhibitor; TSP1, thrombospondin-1.

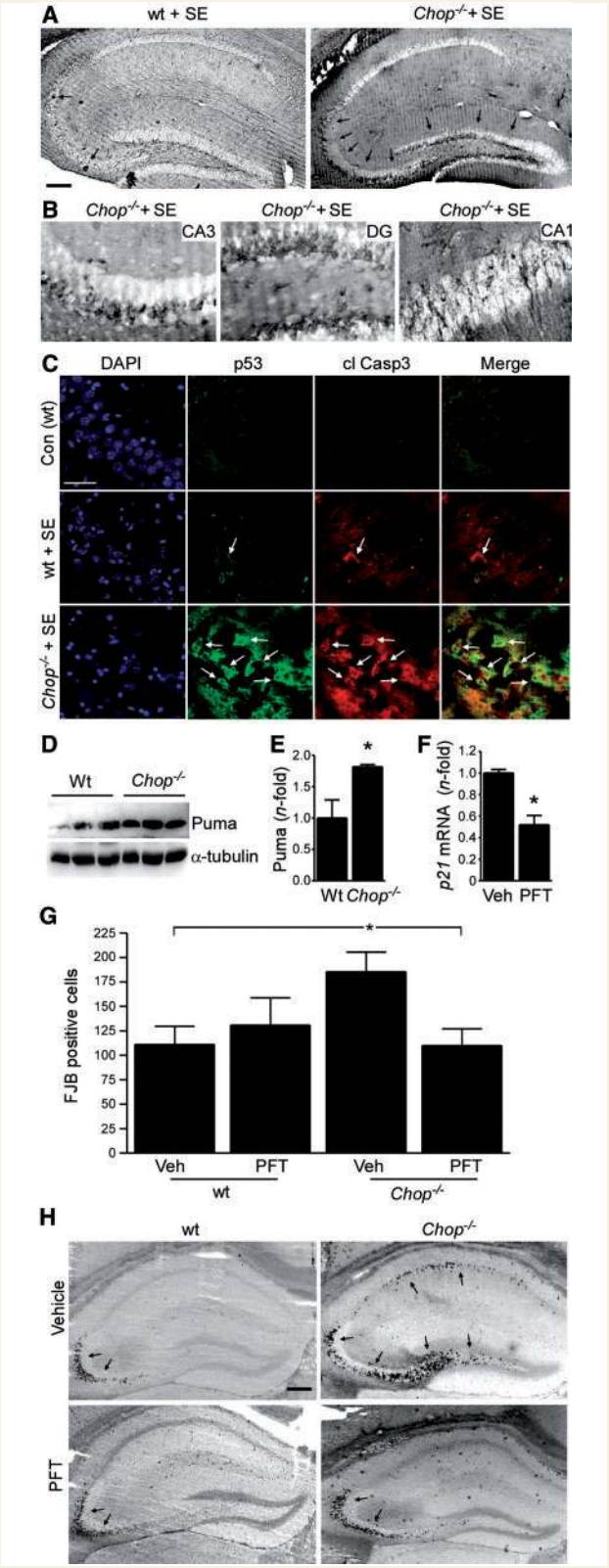

Figure 5 Inhibition of p53 restores seizure-damage to wild-type levels in CHOP-deficient animals. (**A**) Representative photomicrographs showing occasional p53-positive cells in CA3 in wild-type mice 24 h after status epilepticus (arrows), whereas strong p53 staining can be observed in *Chop*$^{-/-}$ mice, particularly in CA3 and the dentate gyrus (DG) (arrows). (**B**) Images (×40 lens) from *Chop*$^{-/-}$ mice showing neuronal and nuclear p53 staining in CA3, CA1 and dentate gyrus 24 h after status epilepticus. (**C**) Immunofluoresence images of the ipsilateral CA3 hippocampal subfield at 24 h showing nucleus (DAPI, blue), p53 (green) and apoptosis marker cleaved caspase 3 (cl Casp3, red) in non-seizure wild-type and wild-type and *Chop*$^{-/-}$ 24 h after status epilepticus. Note only limited p53 and cleaved caspase 3 in wild-type mice after status epilepticus compared with *Chop*$^{-/-}$ mice. Western blot (**D**) and corresponding graph (**E**) showing higher Puma levels in the hippocampus of *Chop*$^{-/-}$ mice compared with wild-type mice 24 h after status epilepticus ($n = 3$/group). α-Tubulin is shown as loading control. (**F**) Graph showing the p53 inhibitor pifithrin-α reduced *p21*$^{WAF/Cip1}$ messenger RNA levels 4 h after status epilepticus ($n = 4$/group). (**G**) Graph showing Fluoro-Jade B-positive cells in hippocampus 72 h after status epilepticus in wild-type and *Chop*$^{-/-}$ mice treated with vehicle or pifithrin-α. Cell death was increased in vehicle-treated *Chop*$^{-/-}$ mice and this was reversed by pifithrin-α ($n = 3$–7/group). (**H**) Representative photomicrographs showing Fluoro-Jade B staining in hippocampus from wild-type and *Chop*$^{-/-}$ mice treated with vehicle or pifithrin-α. Statistically significant differences are indicated by $^{*}P < 0.05$. Scale bar = 250 μm (**A** and **H**), 50 μm (**C**). Data presented as mean ± SEM. DAPI = 4′,6-diamidino-2-phenylindole; FJB = Fluoro-Jade B; PFT = pifithrin-α; SE = status epilepticus; wt = wild-type.

MDM2 is a target of CHOP

The accumulation of p53 protein in *Chop*$^{-/-}$ mice after status epilepticus along with unchanging *p53* messenger RNA is consistent with a failure of the post-translational mechanisms controlling p53 levels. Cellular levels of p53 protein are regulated by the protein product of the murine double minute 2 (*Mdm2*) gene via post-translational ubiquitination and degradation by the proteasome (Toledo and Wahl, 2006). Bioinformatic analysis of the MDM2 promoter using the Algen Promo database (PMID: 11847087; 12824386) revealed putative binding sites for CHOP (Fig. 6A). To investigate whether CHOP can alter the expression of *Mdm2*, we cloned a 2.1-kB fragment containing ~1.9 kb of sequence 5′ to the transcription initiation site of *Mdm2* in the mouse genome into the promoterless pGL3-basic vector (see 'Materials and methods' section). Overexpressing CHOP was sufficient to increase expression of luciferase driven by the MDM2 promoter (Fig. 6A). Also supporting CHOP as a regulator of MDM2, we found *Mdm2* transcript levels increased after status epilepticus in wild-type but not in *Chop*$^{-/-}$ mice (Fig. 6B). MDM2 protein levels were also lower after status epilepticus in *Chop*$^{-/-}$ mice than wild-type animals (Fig. 6C and D). Last, seizure preconditioning increased CHOP and MDM2 levels in wild-type mice but not in *Chop*$^{-/-}$ mice (Fig. 6E–G).

Increased spontaneous seizures and ongoing neurodegeneration after status epilepticus in *Chop*$^{-/-}$ mice

Mice develop spontaneous recurrent seizures within a week of status epilepticus induced by intra-amygdala microinjection of

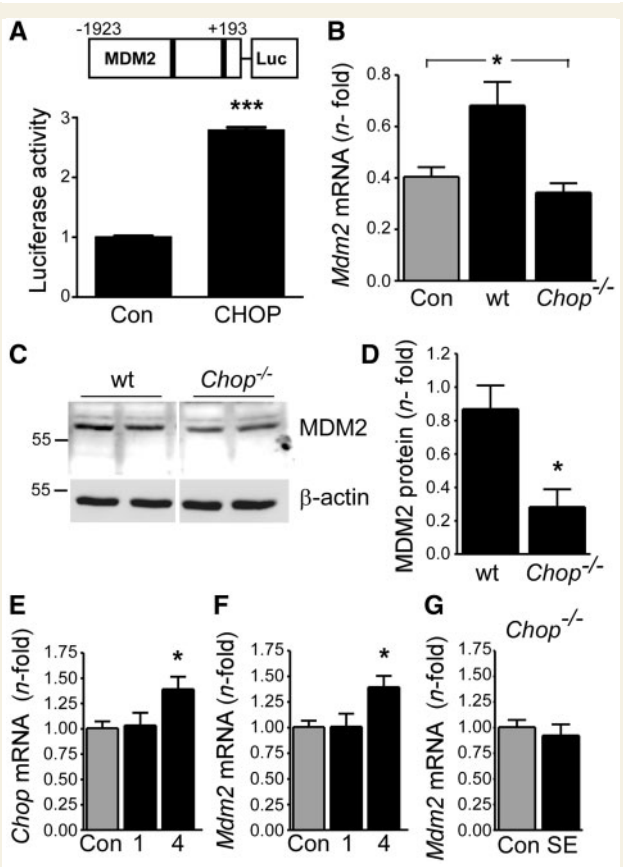

Figure 6 CHOP promotes Mdm2 expression. (**A**) Schematic of the MDM2–pGL3 plasmid showing the cloned *Mdm2* sequence driving the expression of the luciferase gene. The numbers shown are the sequence relative to the transcription initiation site for the first exon of *Mdm2*. The regions with putative C/EBP binding sites are denoted as vertical black bars. Graph: SHSY5y cells were transfected with the MDM2–pGL3 plasmid and the phRL-TK-luc Renilla luciferase plasmid alongside either a CHOP expression plasmid or its empty vector control (Con). After 24 h, cells were lysed, and luciferase activity was monitored ($n = 12$/group). (**B**) *Mdm2* messenger RNA levels in wild-type mice 6 h after status epilepticus when compared with wild-type control and $Chop^{-/-}$ mice 6 h after status epilepticus ($n = 4 – 5$/group). (**C** and **D**) Western blot and corresponding graph showing MDM2 protein levels in wild-type and $Chop^{-/-}$ mice 6 h after status epilepticus ($n = 3$/group). (**E** and **F**) *Chop* and *Mdm2* messenger RNA levels after seizure preconditioning ($n = 5$/group). (**G**) *Mdm2* levels in $Chop^{-/-}$ mice 4 h after preconditioning ($n = 4$/group). Statistically significant differences are indicated by $^{*}P < 0.05$; $^{***}P < 0.001$. Lanes in (**C**) were run on the same gel but were non-contiguous (white lines). Data presented as mean ± SEM. DAPI = 4′,6-diamidino-2-phenylindole; FJB = Fluoro-Jade B; PFT = pifithrin-α; SE = status epilepticus; wt = wild-type.

kainic acid, with a subsequent rise in seizure frequency by 3 weeks (Fig. 7A and see Mouri *et al*., 2008; Jimenez-Mateos *et al*., 2010). During this period, the CA3 subfield develops neuron loss and astrogliosis and is the source of spontaneous seizures (Fig. 7B) (Li *et al*., 2008). Hippocampal lysates from epileptic mice contained higher levels of spliced *Xbp1* but normal levels of ATF4 and cleaved ATF6 (Fig. 7C–E), suggesting that only the survival-promoting IRE1 branch of the unfolded protein response is active in epilepsy (Lin *et al*., 2007).

We next equipped wild-type and $Chop^{-/-}$ mice with EEG telemetry units to investigate whether increased damage after status epilepticus affected later spontaneous seizures, undertaking continuous EEG recordings for 2 weeks. Wild-type mice began experiencing spontaneous seizures 3–4 days after status epilepticus, whereas epileptic seizures emerged earlier in $Chop^{-/-}$ mice (Fig. 7F). $Chop^{-/-}$ mice had more frequent spontaneous seizures than wild-type mice, although the duration of individual seizures, when they occurred, was similar (Fig. 7G–I). No seizures were detected in $Chop^{-/-}$ mice that received only intra-amygdala saline ($n = 2$). Consistent with these data, we noted a tendency towards higher seizure frequency as well as greater mortality in $Chop^{-/-}$ mice during video-only monitoring of generalized tonic–clonic seizures 4 weeks after status epilepticus (Supplementary Fig. 9).

Ongoing cell death was rarely found in the hippocampus of wild-type mice 2 weeks after status epilepticus (Fig. 8A). In contrast, there was substantial ongoing neuronal death in the hippocampus of $Chop^{-/-}$ mice 2 weeks after status epilepticus (Fig. 8A). Reduced neuron counts were also found in the granule cell layer of the dentate gyrus of $Chop^{-/-}$ mice (Fig. 8B).

We next examined performance of wild-type and $Chop^{-/-}$ mice in a simple hippocampus-dependent object–place recognition task (Wimmer *et al*., 2012). Animals were habituated to two objects. The position of one of these objects is then moved before the next trial, which normally produces an increase in time spent with the newly placed object (Wimmer *et al*., 2012). There were no differences in performance of the task between naïve wild-type and naïve $Chop^{-/-}$ mice (Supplementary Fig. 10A–E). Next, we examined the performance of epileptic wild-type and epileptic $Chop^{-/-}$ mice, 3 weeks after status epilepticus. There were no differences in distance travelled or velocity, but both groups of epileptic mice spent less time in open areas during the initial training phase compared with non-seizure control mice (Fig. 8C and Supplementary Fig 10F–I). In contrast, epileptic $Chop^{-/-}$ mice, but not epileptic wild-type mice, displayed a significant deficit in time spent with the novel object, suggesting a memory deficit (Fig. 8D).

Finally, we examined hippocampus from epileptic mice at the end of telemetry monitoring. Western blot analysis showed higher p53 and lower MDM2 levels in $Chop^{-/-}$ mice compared with wild-type animals (Fig. 8E and F).

CHOP is overexpressed in experimental and human temporal lobe epilepsy

Finally, we examined CHOP in experimental and human epilepsy (Fig. 9). CHOP protein levels were higher in the hippocampus of chronically epileptic mice (Fig. 9A and B). In human brain, CHOP was present at low levels in autopsy control hippocampus (Fig. 9C). In contrast, CHOP was detected in all samples of non-sclerotic hippocampus from patients with temporal lobe

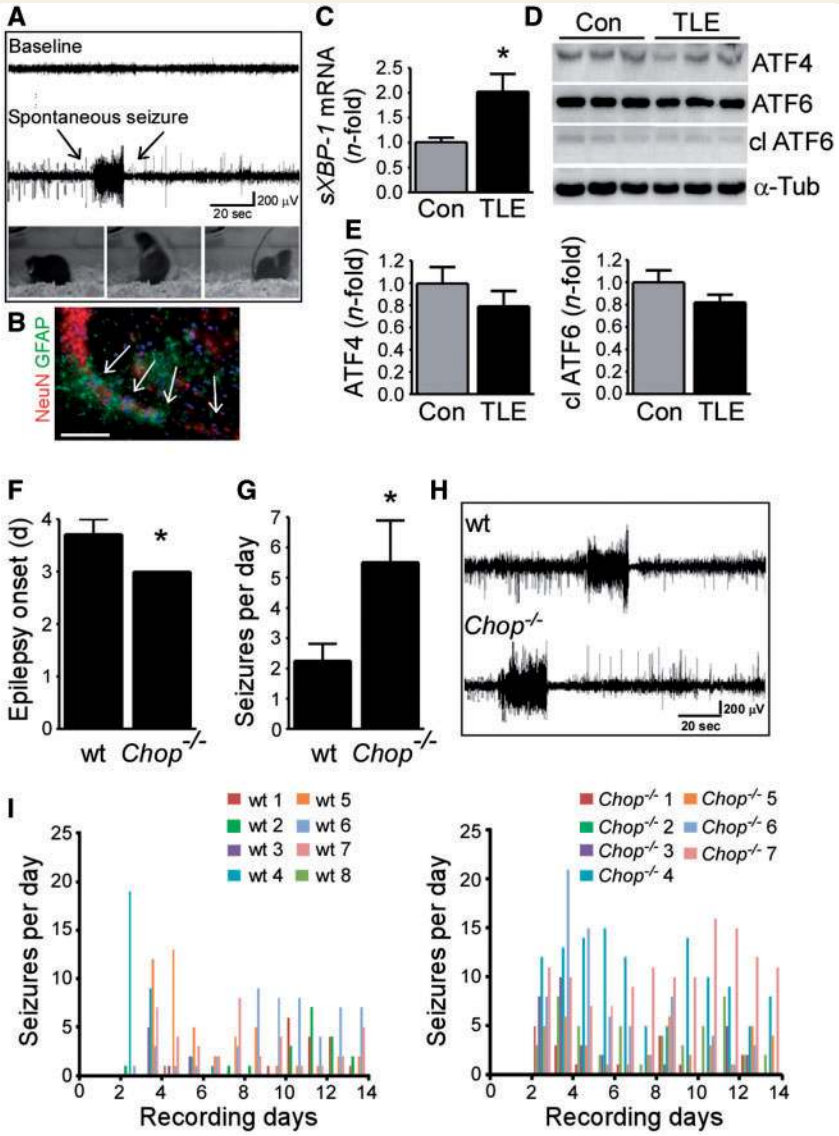

Figure 7 Increased spontaneous seizures in *Chop*$^{-/-}$ mice after status epilepticus. (**A**) Representative telemetry-recorded spontaneous seizure 14 days after status epilepticus. Video stills below show tonic–clonic clinical behaviour. (**B**) Photomicrograph showing ipsilateral CA3 stained for NeuN and glial fibrillary acidic protein (GFAP). (**C**) Increased *Xbp1* splicing in the hippocampus of epileptic mice 14 days after status epilepticus ($n = 4$/group). (**D**) Western blot ($n = 1$ per lane) showing ATF4, ATF6 and cleaved (cl) ATF6 in lysates from epileptic mice. (**E**) Graphs showing levels of ATF4 and cleaved ATF6 in epileptic mice compared with control mice. (**F**) Onset of spontaneous seizures in wild-type and *Chop*$^{-/-}$ mice after status epilepticus ($n = 7$–8/group). (**G**) Spontaneous seizures per day in wild-type and *Chop*$^{-/-}$ mice averaged from 12 days of continuous EEG recording ($n = 7$–8/group). (**H**) Representative EEG traces of spontaneous seizures recorded in wild-type and *Chop*$^{-/-}$ mice. (**I**) Graphs show individual seizures per day in wild-type (wt 1–8) and *Chop*$^{-/-}$ mice (*Chop*$^{-/-}$ 1–7) from days 3 to 14 post status epilepticus. Statistically significant differences are indicated by $^*P < 0.05$. Scale bar = 75 µm. Data presented as mean ± SEM. Con = control; TLE = temporal lobe epilepsy.

epilepsy (Fig. 9C). CHOP levels were not different from autopsy control in sclerotic hippocampus from patients with temporal lobe epilepsy (Fig. 9D). CHOP protein level was also higher in non-sclerotic neocortex from patients with temporal lobe epilepsy compared with autopsy control subjects (Fig. 9E and F). A simulated autopsy delay using mouse brain showed CHOP protein levels in the hippocampus are stable over the period corresponding to the maximal delay in the human control subjects (Supplementary Fig. 11).

Discussion

The present study demonstrates that CHOP is upregulated in surviving neurons and in chronic experimental and human epilepsy. Critically, we show that an absence of CHOP increases neuronal death in models of prolonged seizures. This was associated with a much stronger p53 induction than normal, and reporter assays show CHOP can promote *Mdm2* transcription, which may restrain p53 function. We must be cautious in

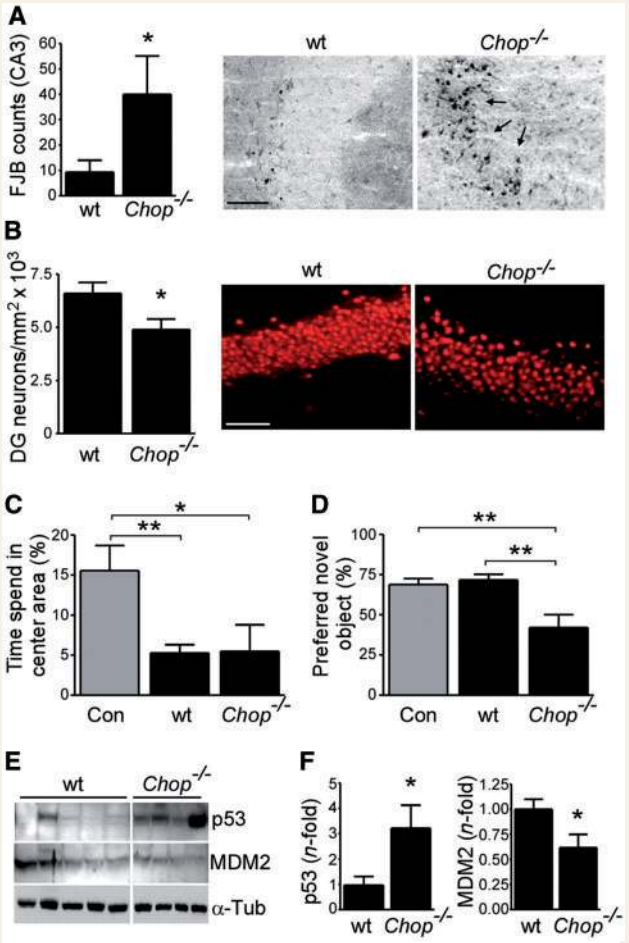

Figure 8 Ongoing neurodegeneration and increased p53 levels in epileptic *Chop*$^{-/-}$ mice. (**A**) Graph and representative photomicrographs showing Fluoro-Jade B (FJB) in the ipsilateral CA3 in epileptic *Chop*$^{-/-}$ mice 14 days after status epilepticus compared with wild-type mice (n = 8–15/group). (**B**) Graph showing neuron density, assessed by NeuN immunohistochemistry, in the dentate gyrus (DG) of epileptic wild-type (wt) and *Chop*$^{-/-}$ mice 14 days after status epilepticus (n = 8–15). *Right*: representative photomicrographs of the blade of the dentate gyrus. (**C**) Graph showing percentage of time spent in the centre area during habituation period of object location memory task. (**D**) Graph showing the percentage preference for the displaced object (n = 10 – 4 per group). (**E** and **F**) Western blots and graphs showing p53 and MDM2 protein levels in epileptic wild-type and *Chop*$^{-/-}$ mice (n = 5–7/group). Statistically significant differences are indicated by $^{*}P < 0.05$. Scale bar = 150 μm (**A**), 50 μm in (**B**). Lanes in (**E**) were run on the same gel but were non-contiguous (white lines). Data presented as mean ± SEM.

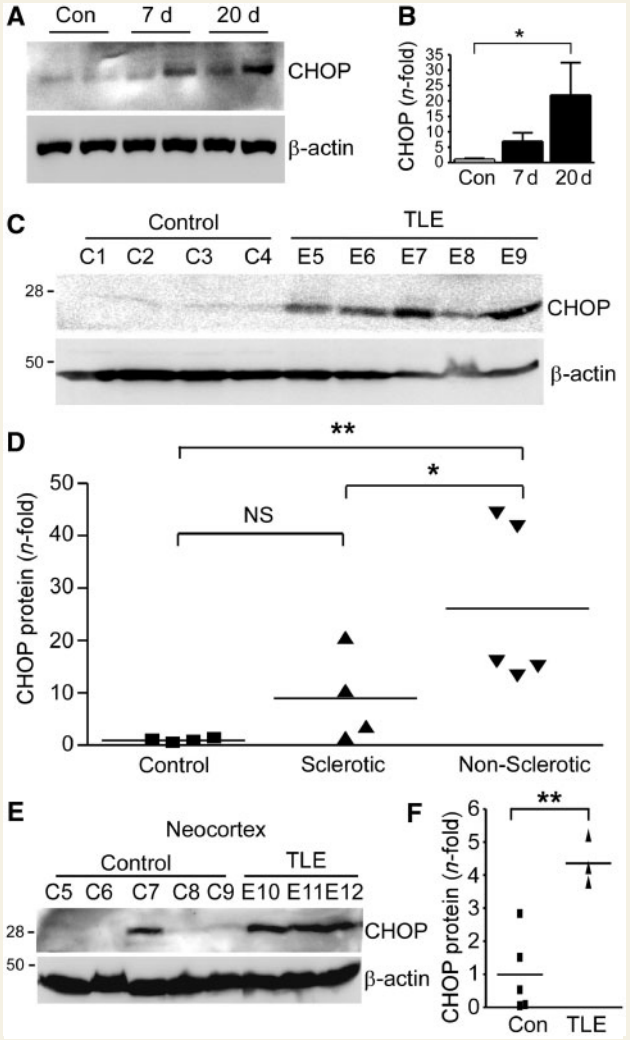

Figure 9 Increased hippocampal levels of CHOP in experimental and human temporal lobe epilepsy. (**A** and **B**) Western blots and graph showing CHOP protein in mice 7 and 20 days after status epilepticus for the ipsilateral hippocampus. β-Actin is shown as loading control (n = 4/group). (**C**) Western blots showing CHOP in autopsy control hippocampus (Control) and non-sclerotic hippocampus from patients with temporal lobe epilepsy (TLE). β-Actin was used as loading control. (**D**) CHOP protein levels in sclerotic and non-sclerotic temporal lobe epilepsy patient hippocampus compared with control mice. (**E** and **F**) Western blot and graph showing CHOP protein in non-sclerotic temporal lobe epilepsy and autopsy control neocortex. Statistically significant differences are indicated by $^{*}P < 0.05$; $^{**}P < 0.01$. Data presented as mean ± SEM. NS = not significant.

assigning clinical importance to any single pathway, but given the exacerbation of damage and protracted neurodegeneration in mice lacking CHOP after status epilepticus, these data indicate that CHOP-inducing agents may be a potential strategy for protection against seizure-induced brain injury and, perhaps, anti-epileptogenesis.

Both endoplasmic reticulum stress and DNA damage are thought to contribute to the pathogenesis of several neurological and neurodegenerative diseases, and CHOP has been proposed as a common effector (Oyadomari and Mori, 2004; Tajiri *et al*., 2004; Puthalakath *et al*., 2007; He *et al*., 2012). The present study demonstrates that CHOP transcript and protein is induced in models of status epilepticus in mice, thus extending previous

work (Murphy *et al*., 2010). An early finding here was that CHOP was induced in damage-resistant subfields of the ipsilateral and contralateral hippocampus and also by brief non-harmful seizures that activate endogenous neuroprotective programmes (Hatazaki *et al*., 2007). Our data are, therefore, not consistent with an exclusively pro-apoptotic role for this transcription factor but instead suggest a context-dependent function for CHOP. We cannot, however, exclude that CHOP may exert a pro- as well as anti-apoptotic effect on the ipsilateral CA3 subfield where damage occurs and where CHOP was also induced. Evidence supporting CHOP as a survival factor was provided by our analysis of *Chop*$^{-/-}$ mice subject to status epilepticus. The standard injury in the model is a lesion restricted to the ipsilateral CA3 subfield (Mouri *et al*., 2008). In *Chop*$^{-/-}$ mice, the ipsilateral CA3 subfield was more damaged than normal, and there was seizure-damage to the ipsilateral CA1 and dentate gyrus and the contralateral hippocampus. The increased vulnerability was independent of the means of seizure induction, also occurring when pilocarpine was used to produce status epilepticus. More prolonged seizures could be a cause of additional damage, but this was excluded by EEG analysis and measurement of activity-regulated and DNA damage-induced gene expression, which was similar to wild-type animals. Taken together, this supports a requirement of CHOP for neuronal survival after status epilepticus.

Our data are compatible with the original function of CHOP as a proto-oncogene (Forus *et al*., 1994) and the survival-promoting functions of CHOP in some models of neuronal injury (Southwood *et al*., 2002; Song *et al*., 2008; Halterman *et al*., 2010). This contrasts studies where CHOP was reported to promote neuronal death (Silva *et al*., 2005; Galehdar *et al*., 2010; Prasanthi *et al*., 2011; Ghosh *et al*., 2012), including after global ischaemia (Tajiri *et al*., 2004) and subarachnoid haemorrhage (He *et al*., 2012). There are examples of a single protein having both pro- and anti-apoptotic functions in brain injury (Beurel and Jope, 2006). Contributions of pro-apoptotic Bcl-2 family proteins to cell death also differ between neurological injuries (Engel *et al*., 2011). The timing and duration of endoplasmic reticulum stress are known to be critical determinants of pro- or anti-apoptotic outcome (Lin *et al*., 2007), and the functions of CHOP may also be context-dependent. However, differences cannot be readily accounted for by the scale or onset-offset of CHOP induction (Tajiri *et al*., 2004; Prasanthi *et al*., 2011; He *et al*., 2012), use of short-interfering RNA versus genetic knockout to modulate CHOP (Tajiri *et al*., 2004; Halterman *et al*., 2010; He *et al*., 2012), and it is not a brain region-specific effect (Tajiri *et al*., 2004; Prasanthi *et al*., 2011). The pro- and anti-apoptotic effects of CHOP may depend on differences in parallel signalling pathways or the duration of activity of individual branches of the unfolded protein response (Lin *et al*., 2007).

The present study provides insight into the mechanism by which CHOP may protect against seizure-induced neuronal death. Microarrays indicated that although the categories of genes changed were similar between wild-type and *Chop*$^{-/-}$ mice after status epilepticus, the fold change of those regulating cell death was much larger in the absence of CHOP. This suggests CHOP modifies the extent to which genes can be transcribed, acting as a 'brake' on overexpression of genes (Jauhiainen *et al*., 2012). The present work goes further, however, and identifies a specific role for CHOP in regulating the p53–MDM2 axis. Induction of p53 contributes to seizure-induced neuronal death (Morrison *et al*., 1996; Engel *et al*., 2010*a*, *b*) and in wild-type mice p53 levels peaked at 24 h and returned to baseline. In contrast, p53 protein levels continued to increase over time in *Chop*$^{-/-}$ mice in line with progression of hippocampal damage. Indeed, neurodegeneration continued for weeks after status epilepticus in *Chop*$^{-/-}$ mice. The additional damage in *Chop*$^{-/-}$ mice was largely prevented by a p53 inhibitor, supporting p53 involvement. Induction of Puma, the effector of p53-induced neuronal death after seizures (Engel *et al*., 2010*a*), was also higher in *Chop*$^{-/-}$ mice. An important mechanism regulating cellular levels of p53 involves MDM2. The ubiquitin-proteosome system is the major non-lysosomal pathway for degradation of proteins in cells, including p53, and MDM2 mediates p53 ubiquitination followed by degradation via the proteasome (Lavin and Gueven, 2006; Toledo and Wahl, 2006). Reporter experiments here established CHOP can drive MDM2 expression, and we found that MDM2 was not induced after status epilepticus in CHOP-deficient mice. Thus, the supramaximal p53 levels in *Chop*$^{-/-}$ mice may result from a failure of this mechanism to restrain p53 (summarized in Supplementary Fig. 12). However, MDM2 levels were normal in naïve *Chop*$^{-/-}$ mice, suggesting that CHOP is not involved in maintenance of basal MDM2 levels. Together, these results provide a mechanistic explanation for the damage-vulnerable phenotype in *Chop*$^{-/-}$ mice and add CHOP to the network of proteins that regulate the p53–MDM2 axis (Lavin and Gueven, 2006).

The present study found higher CHOP levels in both experimental and human temporal lobe epilepsy. These are the first data on CHOP in epilepsy. If CHOP protects neurons from seizure-induced neuronal death, then we can speculate that the raised CHOP levels in hippocampus and neocortex in temporal lobe epilepsy patient material may be an adaptation to recurrent seizures that could limit further neuron loss. Consistent with this idea, CHOP levels were not elevated in sclerotic hippocampus where cell death may be ongoing (Mathern *et al*., 2002; Bernasconi and Bernhardt, 2010; Henshall and Meldrum, 2012). The high levels of CHOP in chronic epilepsy where little or no ongoing cell death occurs, along with the continued degeneration of the hippocampus in *Chop*$^{-/-}$ mice after status epilepticus, support CHOP serving an anti-apoptotic function in epilepsy. However, as with previous studies in ischaemia (Moskowitz *et al*., 2010), we must be cautious before assigning clinical importance to any single pathway.

In summary, the present study identifies CHOP as important for neuronal survival after status epilepticus and finds CHOP is upregulated in human epilepsy. CHOP may indirectly promote neuronal survival by restraining p53 induction via MDM2 upregulation. Given that excitotoxicity underlies various neurological and neurodegenerative diseases, these data caution against targeting CHOP for neuroprotection in acute and chronic diseases of the central nervous system and suggest CHOP delivery may protect against seizure-induced neuronal death and, perhaps, anti-epileptogenesis.

Acknowledgements

The authors thank Alison Murphy (Conway Institute) and Alicia Tomico for excellent technical assistance. They thank the Brain and Tissue Bank for Developmental Disorders at the University of Maryland, Baltimore, MD, USA. We also thank Julika Pitsch and Albert Becker for advice on the pilocarpine model.

Funding

Health Research Board (PD/2009/31 to T.E. and HRA_POR/2011/41 to D.C.H.); Science Foundation Ireland (08/IN.1./B1875 to D.C.H.); Spanish Ministry of Science MEC/MICINN/MINECO, CiberNed, and Fundación Ramón Areces.

Supplementary material

Supplementary material is available at *Brain* online.

References

Acharya MM, Hattiangady B, Shetty AK. Progress in neuroprotective strategies for preventing epilepsy. Prog Neurobiol 2008; 84: 363–404.

Bernasconi N, Bernhardt BC. Temporal lobe epilepsy is a progressive disorder. Nat Rev Neurol 2010; 6: 1.

Beurel E, Jope RS. The paradoxical pro- and anti-apoptotic actions of GSK3 in the intrinsic and extrinsic apoptosis signaling pathways. Prog Neurobiol 2006; 79: 173–89.

Chang BS, Lowenstein DH. Epilepsy. N Engl J Med 2003; 349: 1257–66.

Chen CM, Wu CT, Chiang CK, Liao BW, Liu SH. C/EBP homologous protein (CHOP) deficiency aggravates hippocampal cell apoptosis and impairs memory performance. PLoS One 2012; 7: e40801.

Chigurupati S, Wei Z, Belal C, Vandermey M, Kyriazis GA, Arumugam TV, et al. The homocysteine-inducible endoplasmic reticulum stress protein counteracts calcium store depletion and induction of CCAAT enhancer-binding protein homologous protein in a neurotoxin model of Parkinson disease. J Biol Chem 2009; 284: 18323–33.

Chihara Y, Ueda Y, Doi T, Willmore LJ. Role of endoplasmic reticulum stress in the amygdaloid kindling model of rats. Neurochem Res 2011; 36: 1834–9.

Cui H, Hu B, Li T, Ma J, Alam G, Gunning WT, et al. Bmi-1 is essential for the tumorigenicity of neuroblastoma cells. Am J Pathol 2007; 170: 1370–8.

Engel T, Gomez-Villafuertes R, Tanaka K, Mesuret G, Sanz-Rodriguez A, Garcia-Huerta P, et al. Seizure suppression and neuroprotection by targeting the purinergic P2X7 receptor during status epilepticus in mice. FASEB J 2012; 26: 1616–28.

Engel T, Murphy BM, Hatazaki S, Jimenez-Mateos EM, Concannon CG, Woods I, et al. Reduced hippocampal damage and epileptic seizures after status epilepticus in mice lacking proapoptotic Puma. FASEB J 2010a; 24: 853–61.

Engel T, Plesnila N, Prehn JH, Henshall DC. In vivo contributions of BH3-only proteins to neuronal death following seizures, ischemia, and traumatic brain injury. J Cereb Blood Flow Metab 2011; 31: 1196–210.

Engel T, Tanaka K, Jimenez-Mateos EM, Caballero-Caballero A, Prehn JH, Henshall DC. Loss of p53 results in protracted electrographic seizures and development of an aggravated epileptic phenotype following status epilepticus. Cell Death Dis 2010b; 1: e79.

Falconer MA. Mesial temporal (Ammon's horn) sclerosis as a common cause of epilepsy. Aetiology, treatment, and prevention. Lancet 1974; 2: 767–70.

Forus A, Florenes VA, Maelandsmo GM, Fodstad O, Myklebost O. The protooncogene CHOP/GADD153, involved in growth arrest and DNA damage response, is amplified in a subset of human sarcomas. Cancer Genet Cytogenet 1994; 78: 165–71.

Fujikawa DG. Neuroprotective strategies in status epilepticus. In: Wasterlain CG, Treiman DM, editors. Status epilepticus: mechanisms and management. Cambridge: MIT Press; 2006. p. 463–480.

Galehdar Z, Swan P, Fuerth B, Callaghan SM, Park DS, Cregan SP. Neuronal apoptosis induced by endoplasmic reticulum stress is regulated by ATF4-CHOP-mediated induction of the Bcl-2 homology 3-only member PUMA. J Neurosci 2010; 30: 16938–48.

Ghosh AP, Klocke BJ, Ballestas ME, Roth KA. CHOP potentially co-operates with FOXO3a in neuronal cells to regulate PUMA and BIM expression in response to ER stress. PLoS One 2012; 7: e39586.

Gow A, Wrabetz L. CHOP and the endoplasmic reticulum stress response in myelinating glia. Curr Opin Neurobiol 2009; 19: 505–10.

Halterman MW, Gill M, DeJesus C, Ogihara M, Schor NF, Federoff HJ. The endoplasmic reticulum stress response factor CHOP-10 protects against hypoxia-induced neuronal death. J Biol Chem 2010; 285: 21329–40.

Hatazaki S, Bellver-Estelles C, Jimenez-Mateos EM, Meller R, Bonner C, Murphy N, et al. Microarray profile of seizure damage-refractory hippocampal CA3 in a mouse model of epileptic preconditioning. Neuroscience 2007; 150: 467–77.

He Z, Ostrowski RP, Sun X, Ma Q, Huang B, Zhan Y, et al. CHOP silencing reduces acute brain injury in the rat model of subarachnoid hemorrhage. Stroke 2012; 43: 484–90.

Henshall DC, Meldrum BS. Cell death and survival mechanisms after single and repeated brief seizures. In: Jasper's basic mechanisms of the epilepsies. 4th edn. Bethesda, MD: Oxford University Press; 2012. p. 262–76.

Henshall DC, Murphy BM. Modulators of neuronal cell death in epilepsy. Curr Opin Pharmacol 2008; 8: 75–81.

Hetz C. The unfolded protein response: controlling cell fate decisions under ER stress and beyond. Nat Rev Mol Cell Biol 2012; 13: 89–102.

Jauhiainen A, Thomsen C, Strombom L, Grundevik P, Andersson C, Danielsson A, et al. Distinct cytoplasmic and nuclear functions of the stress induced protein DDIT3/CHOP/GADD153. PLoS One 2012; 7: e33208.

Jimenez-Mateos EM, Engel T, Merino-Serrais P, McKiernan RC, Tanaka K, Mouri G, et al. Silencing microRNA-134 produces neuroprotective and prolonged seizure-suppressive effects. Nat Med 2012; 18: 1087–94.

Jimenez-Mateos EM, Mouri G, Conroy RM, Henshall DC. Epileptic tolerance is associated with enduring neuroprotection and uncoupling of the relationship between CA3 damage, neuropeptide Y rearrangement and spontaneous seizures following intra-amygdala kainic acid-induced status epilepticus in mice. Neuroscience 2010; 171: 556–65.

Kitao Y, Ozawa K, Miyazaki M, Tamatani M, Kobayashi T, Yanagi H, et al. Expression of the endoplasmic reticulum molecular chaperone (ORP150) rescues hippocampal neurons from glutamate toxicity. J Clin Invest 2001; 108: 1439–50.

Kotloski R, Lynch M, Lauersdorf S, Sutula T. Repeated brief seizures induce progressive hippocampal neuron loss and memory deficits. Prog Brain Res 2002; 135: 95–110.

Lavin MF, Gueven N. The complexity of p53 stabilization and activation. Cell Death Differ 2006; 13: 941–50.

Li T, Ren G, Lusardi T, Wilz A, Lan JQ, Iwasato T, et al. Adenosine kinase is a target for the prediction and prevention of epileptogenesis in mice. J Clin Invest 2008; 118: 571–82.

Lin JH, Li H, Yasumura D, Cohen HR, Zhang C, Panning B, et al. IRE1 signaling affects cell fate during the unfolded protein response. Science 2007; 318: 944–9.

Mathern GW, Adelson PD, Cahan LD, Leite JP. Hippocampal neuron damage in human epilepsy: Meyer's hypothesis revisited. Prog Brain Res 2002; 135: 237–51.

McKiernan RC, Jimenez-Mateos EM, Bray I, Engel T, Brennan GP, Sano T, et al. Reduced mature microRNA levels in association with

Dicer loss in human temporal lobe epilepsy with hippocampal sclerosis. PLoS One 2012; 7: e35921.
Milhavet O, Martindale JL, Camandola S, Chan SL, Gary DS, Cheng A, et al. Involvement of Gadd153 in the pathogenic action of presenilin-1 mutations. J Neurochem 2002; 83: 673–81.
Moon DO, Park SY, Choi YH, Ahn JS, Kim GY. Guggulsterone sensitizes hepatoma cells to TRAIL-induced apoptosis through the induction of CHOP-dependent DR5: involvement of ROS-dependent ER-stress. Biochem Pharmacol 2011; 82: 1641–50.
Morrison RS, Wenzel HJ, Kinoshita Y, Robbins CA, Donehower LA, Schwartzkroin PA. Loss of the p53 tumor suppressor gene protects neurons from kainate-induced cell death. J Neurosci 1996; 16: 1337–45.
Moskowitz MA, Lo EH, Iadecola C. The science of stroke: mechanisms in search of treatments. Neuron 2010; 67: 181–98.
Mouri G, Jimenez-Mateos E, Engel T, Dunleavy M, Hatazaki S, Paucard A, et al. Unilateral hippocampal CA3-predominant damage and short latency epileptogenesis after intra-amygdala microinjection of kainic acid in mice. Brain Res 2008; 1213: 140–51.
Murphy BM, Engel T, Paucard A, Hatazaki S, Mouri G, Tanaka K, et al. Contrasting patterns of Bim induction and neuroprotection in Bim-deficient mice between hippocampus and neocortex after status epilepticus. Cell Death Differ 2010; 17: 459–68.
Oyadomari S, Mori M. Roles of CHOP/GADD153 in endoplasmic reticulum stress. Cell Death Differ 2004; 11: 381–9.
Pelletier MR, Wadia JS, Mills LR, Carlen PL. Seizure-induced cell death produced by repeated tetanic stimulation in vitro: possible role of endoplasmic reticulum calcium stores. J Neurophysiol 1999; 81: 3054–64.
Prasanthi JR, Larson T, Schommer J, Ghribi O. Silencing GADD153/CHOP gene expression protects against Alzheimer's disease-like pathology induced by 27-hydroxycholesterol in rabbit hippocampus. PLoS One 2011; 6: e26420.
Puthalakath H, O'Reilly LA, Gunn P, Lee L, Kelly PN, Huntington ND, et al. ER stress triggers apoptosis by activating BH3-only protein Bim. Cell 2007; 129: 1337–49.
Reijonen S, Putkonen N, Norremolle A, Lindholm D, Korhonen L. Inhibition of endoplasmic reticulum stress counteracts neuronal cell death and protein aggregation caused by N-terminal mutant huntingtin proteins. Exp Cell Res 2008; 314: 950–60.
Ron D, Habener JF. CHOP, a novel developmentally regulated nuclear protein that dimerizes with transcription factors C/EBP and LAP and functions as a dominant-negative inhibitor of gene transcription. Genes Dev 1992; 6: 439–53.
Rouschop KM, van den Beucken T, Dubois L, Niessen H, Bussink J, Savelkouls K, et al. The unfolded protein response protects human tumor cells during hypoxia through regulation of the autophagy genes MAP1LC3B and ATG5. J Clin Invest 2010; 120: 127–41.
Silva RM, Ries V, Oo TF, Yarygina O, Jackson-Lewis V, Ryu EJ, et al. CHOP/GADD153 is a mediator of apoptotic death in substantia nigra dopamine neurons in an in vivo neurotoxin model of parkinsonism. J Neurochem 2005; 95: 974–86.
Sloviter RS. Progress on the issue of excitotoxic injury modification vs. real neuroprotection; implications for post-traumatic epilepsy. Neuropharmacology 2011; 61: 1048–50.
Sokka AL, Putkonen N, Mudo G, Pryazhnikov E, Reijonen S, Khiroug L, et al. Endoplasmic reticulum stress inhibition protects against excitotoxic neuronal injury in the rat brain. J Neurosci 2007; 27: 901–8.
Song B, Scheuner D, Ron D, Pennathur S, Kaufman RJ. Chop deletion reduces oxidative stress, improves beta cell function, and promotes cell survival in multiple mouse models of diabetes. J Clin Invest 2008; 118: 3378–89.
Southwood CM, Garbern J, Jiang W, Gow A. The unfolded protein response modulates disease severity in Pelizaeus-Merzbacher disease. Neuron 2002; 36: 585–96.
Szegezdi E, Logue SE, Gorman AM, Samali A. Mediators of endoplasmic reticulum stress-induced apoptosis. EMBO Rep 2006; 7: 880–5.
Tabas I, Ron D. Integrating the mechanisms of apoptosis induced by endoplasmic reticulum stress. Nat Cell Biol 2011; 13: 184–90.
Tajiri S, Oyadomari S, Yano S, Morioka M, Gotoh T, Hamada JI, et al. Ischemia-induced neuronal cell death is mediated by the endoplasmic reticulum stress pathway involving CHOP. Cell Death Differ 2004; 11: 403–15.
Toledo F, Wahl GM. Regulating the p53 pathway: in vitro hypotheses, in vivo veritas. Nat Rev Cancer 2006; 6: 909–23.
Wimmer ME, Hernandez PJ, Blackwell J, Abel T. Aging impairs hippocampus-dependent long-term memory for object location in mice. Neurobiol Aging 2012; 33: 2220–4.
Xu C, Bailly-Maitre B, Reed JC. Endoplasmic reticulum stress: cell life and death decisions. J Clin Invest 2005; 115: 2656–64.
Yamamoto A, Murphy N, Schindler CK, So NK, Stohr S, Taki W, et al. Endoplasmic reticulum stress and apoptosis signaling in human temporal lobe epilepsy. J Neuropathol Exp Neurol 2006; 65: 217–25.
Zinszner H, Kuroda M, Wang X, Batchvarova N, Lightfoot RT, Remotti H, et al. CHOP is implicated in programmed cell death in response to impaired function of the endoplasmic reticulum. Genes Dev 1998; 12: 982–95.